Detection of electrostatic forces with an atomic force microscope: Analytical and experimental dynamic force curves in the nonlinear regime

R. Dianoux,[1,2,*] F. Martins,[1] F. Marchi,[3,4,†] C. Alandi,[1] F. Comin,[1] and J. Chevrier,[1,3,4]
[1]*ESRF, Boîte Postale 220, 38043 Grenoble cedex 9, France*
[2]*CEA Grenoble, DRFMC/SP2M/SiNaPS, 17 rue des Martyrs, 38054 Grenoble cedex 9, France*
[3]*CNRS/LEPES, 25 avenue des Martyrs, 38042 Grenoble cedex 9, France*
[4]*Université Joseph Fourier, Boîte Postale 53, 38041 Grenoble cedex 9, France*
(Received 14 February 2003; published 1 July 2003)

Dynamic force curves of an atomic force microscope in the presence of attractive van der Waals and electrostatic forces are analytically treated using a variational method taking into account nonlinear tip-sample coupling. This approach allows describing and understanding the motion of a voltage-biased tip observed in experimental approach-retract curves in dynamic mode. The solutions predict a hysteretic behavior in the force curves for both amplitude and phase of oscillation. This hysteresis diminishes and disappears with increasing tip-sample voltage. The tip-surface system is modeled as a plane capacitor with an effective area of interaction. The analytical solution clearly accounts for the apparent height measured in topographical scanning due to the presence of charges on the sample. It also furnishes an estimation of the quantity of excess charges on the sample surface measured in the experiment. There, an estimated 360 electrons were injected into a SiO_2 surface. Additionally, at the onset of electrostatic coupling, an abrupt transition from intermittent contact to noncontact regime is experimentally evidenced by a jump of the phase from one branch of solution to the other. This phase contrast represents an easy way to distinguish and to choose between intermittent contact and noncontact regime.

DOI: 10.1103/PhysRevB.68.045403 PACS number(s): 07.79.Lh, 68.37.Ps, 73.25.+i, 87.64.Dz

I. INTRODUCTION

Injection and detection of localized charges in nanostructures, on or below the surface, are the key issues in fields such as mesoscopy or nanoelectronics. The atomic force microscope (AFM)[1] is in this respect an instrument of choice to probe the surfaces at the nanometer scale in a nondestructive way. Its versatility allows investigating local topographical and mechanical properties in contact regime[2] as well as in dynamic regime of operation. In dynamic AFM, the cantilever is excited near its resonant frequency, and information on the tip-sample interaction is retrieved through the amplitude and the phase of the cantilever motion. Inelastic,[3,4] magnetic,[5] and electrical[6,7] properties of both conductors and dielectrics[8,9] have been studied in this regime. Using a conductive tip, it is possible to electrically bias the oscillating tip with respect to the sample and to probe the long-range electrostatic interactions [electrostatic force microscopy (EFM)].[10,11] Moreover, the AFM has been shown to be capable of charge injection[12,13] and detection of only a few excess charges.[12–16]

However, a quantitative charge determination is delicate due to the intermixing of Coulomb and surface potentials. Topography may play a significant role in the EFM signal.[15] To overcome this challenge, we have concentrated our studies on a nonscanning method. These are dynamic force curves, in which the oscillating AFM probe is successively approached and retracted from the surface, thus probing long-range electrostatic forces.

A partially nonlinear description of the tip motion is necessary to explain experimental dynamic force curves. It supposes that the tip probes a strongly anharmonic potential, but maintains a harmonic motion. Additionally, we have chosen a plane-plane capacitor geometry for the tip-surface system to calculate the electrostatic force between the tip and the sample. This plane-capacitor approximation is in excellent agreement with the experimental data, and allows a direct estimation of the number of injected charges on the surface.[17] The transition between states of oscillation (intermittent contact to noncontact regimes) induced by electrostatic interaction is also experimentally shown. It is the source for a strong phase contrast and possibly imaging instabilities,[18] and underlines the importance of dynamic force curves to choose a stable regime of operation.

II. ANALYTICAL DYNAMIC FORCE CURVES

In dynamic AFM, the tip is mechanically set into oscillation by a bimorph. In this work, we consider the excitation at or near the fundamental resonant frequency. The system can in this case be modeled as a forced, damped, harmonic oscillator, nonlinearly perturbed by the presence of the surface, but nevertheless maintaining an harmonic response.[19–21] Nonlinear tip-sample interactions influence both the amplitude of oscillation and the phase difference between the stimulation and the detected signal, providing information on material properties such as local stiffness[22] and energy dissipation.[3] In particular, a conductive tip is sensitive to long-range, attractive or repulsive electrostatic forces, which can be controlled by an external dc voltage difference applied between the tip and the sample (in the following referred to as V_{EFM}).

In the general case, two regimes of interaction appear,[23] which can be discriminated by the phase of oscillation vs tip-sample separation (dynamic force curves):[24]

 ©2003 The American Physical Society

(1) In the intermittent contact (IC) regime, the tip shortly comes into contact during the oscillation period. This regime is characterized by a monotonous increase of the phase with decreasing distance in dynamic force curves.

(2) In the noncontact (NC) regime, the tip never touches the surface, i.e., it never probes repulsive forces during an oscillation period. This regime can be recognized in the monotonous decrease of the phase with decreasing distance in dynamic force curves.

One can choose the desired regime by adjusting the parameters such as the amplitude of free oscillation or the frequency shift below the free resonance. Both regimes are capable of imaging surface topography. Nevertheless, NC regime has shown to be more suitable to probe electrostatic interactions because it reduces the influence of the tip on charge distribution on the surface. Moreover, in IC regime, the dominant interaction is repulsive, leaving the system less sensitive to electrostatic forces. In the following, only the noncontact situation is analytically treated.

The analytical description follows Nony and co-workers.[24] The tip probes an attractive Van der Waals force to which we add an electrostatic force. We suppose a flat surface (z-rms roughness less than 2 nm) and homogeneous properties of the sample surface. Based on analytical expressions, we study the influence of the tip-sample interaction on amplitude and phase of the tip oscillation with the distance.

The tip motion is sensitive to the gradient of the force in the vertical direction, $\partial F/\partial z$, itself proportional to the second derivative of the capacitance $C''(z)=\partial^2 C/\partial z^2$:

$$\frac{\partial F_z}{\partial z}=C''(z)\frac{V_{EFM}^2}{2}. \tag{1}$$

Notably, V_{EFM} includes the surface potential of the sample, which is a constant only depending on the material. Therefore, it will be omitted in the following. We propose a plane-plane capacitor model to describe this additional electrostatic interaction between the tip and the surface. The expression of $C''(z)$ in this case is

$$C''(z)=2\frac{\epsilon_0 S}{z^3}, \tag{2}$$

where ϵ_0 is the dielectric constant of vacuum and S is the plate area. Considering the real tip-sample geometry, this approximation may seem too rough. However, our mode of operation (interleave mode, during which the tip-sample distance is kept constant) allows us to determine an effective area of the plates of the plane capacitor. Indeed, Hudlet *et al.*[25] calculate the capacitive force vs tip-sample separation, for realistic tip geometry of a truncated cone with a sphere at its apex. An adjustment of the plate area of the plane capacitor is made, so that values of both models coincide at the chosen lift height, here 100 nm. The plot of the calculated $C''(z)$ curves is shown in Fig. 1. The two models coincide for a plate area corresponding to a disc 100 nm in diameter. This value is reasonable, given the geometry of the tip: truncated cone 14 μm in height and 10° half angle, with a sphere at its apex 35 nm in radius (manufacturer's data, see below). It reflects the fact that at this lift height, not only the sphere is interacting with the surface but also the upper part of the cone.

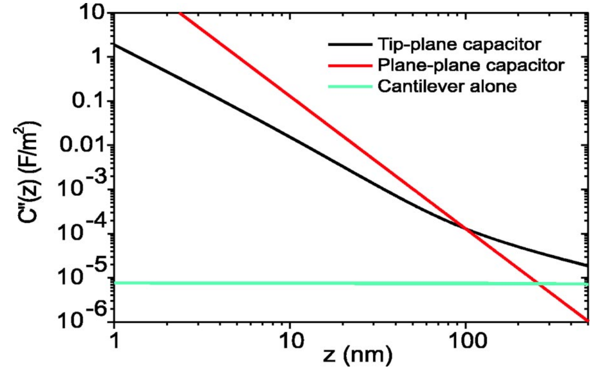

FIG. 1. (Color online) Second derivative of the capacitance $C''(z)$ vs plate distance for two tip-sample models. The plate area of the plane-capacitor model has been set to coincide with the value of the truncated cone-plane model at a separation of 100 nm. Worth noting is the negligible contribution to $C''(z)$ of the cantilever alone (light gray line), modeled at a distance of 14 μm from the surface.

Figure 1 demonstrates that the influence of the capacitance of the cantilever (modeled as plane-plane capacitor at a distance of 14 μm from the sample surface) is negligible. If the total capacitance of the cantilever is large, its variation with the tip-sample distance (typically a few hundreds of nanometers), on the other hand, is very limited, and so is the second derivative. This result has also been emphasized in Ref. 26.

Van der Waals interaction occurs at very small spacing, typically a few nanometers, where the tip can reasonably be modeled as a sphere. The plane-sphere interaction potential is given by the expression (3) from Ref. 27:

$$U_{Waals}=\frac{HR}{6D}, \tag{3}$$

where H is the Hamaker constant, R is the tip radius, and D is tip-surface distance. The additional, electrostatic term provides

$$U_{elec}=\frac{1}{2}CV_{EFM}^2=\frac{\epsilon_0 S}{2D}V_{EFM}^2, \tag{4}$$

where V_{EFM} is the tip voltage, ϵ_0 is the dielectric constant, and S is the effective tip area. Then, the total tip-surface interaction is given by

$$U_{int}=U_{Waals}+U_{elec}=\left(\frac{HR}{6}+\frac{\epsilon_0 S}{2}V_{EFM}^2\right)\frac{1}{D}. \tag{5}$$

From a variational method, based on the principle of least action,[24] we obtain the following expressions that connect the amplitude and the phase of oscillation with the distance:

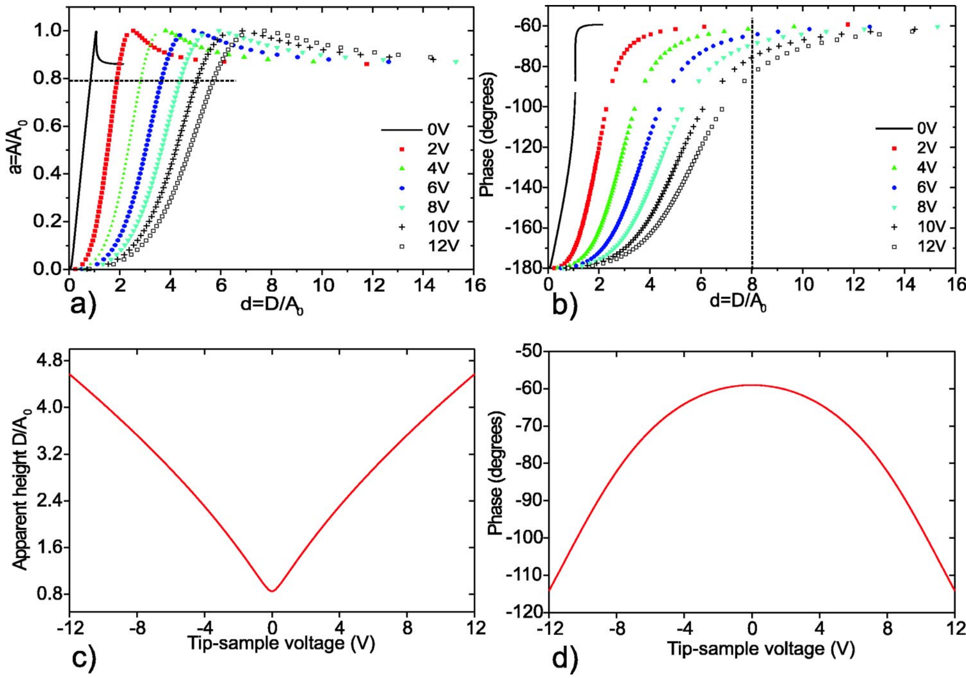

FIG. 2. (Color online) (a) and (b) are, respectively, plots of the theoretical expressions (6) and (7) for different voltages V_{EFM}. Amplitude and tip-sample distance are normalized by the free amplitude of oscillation at the resonance A_0. The parameters used are $u=0.9988$, $A_0=14$ nm, $k_c=3.7\ \mathrm{Nm}^{-1}$, $R=20$ nm, $H=2\times10^{-19}$ J, $K=250$, $k_{Waals}=6.57\times10^{-5}$, and $k_{elec}=3.42\times10^{-3}\ \mathrm{V}^{-2}$. (c) depicts the average tip-surface distance for different voltages at an amplitude setpoint of $a=0.8$. (d) shows the phase shift between the excitation and the detected signal for different voltages at a constant distance $d=8$.

$$d_{A\pm}=\sqrt{a^2+\left(2\frac{k_{Waals}+k_{elec}V_{EFM}^2}{(1-u^2)\mp\frac{1}{K}\sqrt{\frac{1}{a^2}-u^2}}\right)^{2/3}}, \tag{6}$$

$$\phi_{A\pm}=atan\left(\frac{u}{K(u^2-1)+2K\frac{k_{Waals}+k_{elec}V_{EFM}^2}{(d_{A\pm}^2-a^2)^{3/2}}}\right), \tag{7}$$

where A is the amplitude of oscillation, A_0 is the amplitude of free oscillation at the resonant frequency ν_0, $a=A/A_0$ is the reduced amplitude, $d_{A\pm}=D/A_0$ is the reduced distance, $\phi_{A\pm}$ is the phase between excitation and motion of the oscillator, ν is the frequency of the excitation signal, $u=\nu/\nu_0$ is the reduced frequency, K is the quality factor of the oscillator, k_c is the cantilever stiffness, $k_{Waals}=HR/6k_cA_0^3$ is a dimensionless parameter related with van der Waals forces, and $k_{elec}V_{EFM}^2=(\epsilon_0 S/2k_cA_0^3)V_{EFM}^2$ is a dimensionless parameter related with electrostatic forces.

Equations (6) and (7) describe the evolution of the tip motion (amplitude and phase of oscillation) vs tip-sample separation during a force curve for a biased AFM probe. A force curve reflects the contribution of the different forces depending on the tip-surface distance. In practice, to record a force curve, the scan is stopped, the tip is fixed above a chosen area, and the feedback loop is turned off. While the cantilever is excited near its fundamental resonance frequency, it is approached towards the surface by a defined distance, and then retracted, both at a constant speed.

With such force curves, one can unambiguously determine the working regime (IC or NC), and hence adjust the external parameters to choose the desired regime. This way, one can specifically probe long-range attractive forces in noncontact, or short-range repulsive forces in intermittent contact. For both dynamic force curves in amplitude and phase, the resolution provides two branches of solutions, so that bistable situations can occur. Experimentally, a hysteretic behavior is observable, depending on whether the tip is approaching or retracting from the surface. Attention must be drawn on the term u, i.e., the ratio between frequencies of excitation and resonance. If $u=1$, as illustrated in Eqs. (6) and (7), the system does not exhibit two branches of solutions, and hysteresis does not occur. Equations (6) and (7) are plotted in Fig. 2 as a function of the tip-sample distance for different tip-sample voltages.

The hysteretic behavior of the tip motion, clearly apparent in Figs. 2(a) and 2(b) (respectively, amplitude and phase vs distance) at low voltages, diminishes and disappears with increasing voltage, whereas the interaction spans over larger distances. This behavior is illustrated in Figs. 2(c) and 2(d), which are, respectively, plots of the apparent height and phase of oscillation as a function of the tip-sample voltage. The effective height is obtained by considering that for topography, the AFM maintains a constant amplitude (also referred to as amplitude setpoint). The horizontal, dashed line in Fig. 2(a) schematically represents this setpoint, which is arbitrarily set at 80% of the free amplitude. On the other hand, phase is recorded at a constant tip-sample distance. The phase vs voltage graph is therefore plotted along the vertical, dashed line in Fig. 2(b), at a distance of $d=8$ times the free amplitude, that is, ≈ 100 nm. The parabolic behavior of the plot confirms the validity of the plane capacitance model. However, this behavior is lost at smaller values of d. It is worth noting that both curves attain their extremum for $V_{EFM}=0$.

To continue the discussion, we assume that expression (4) is still valid for a silicon sample with a thin silicon-dioxide

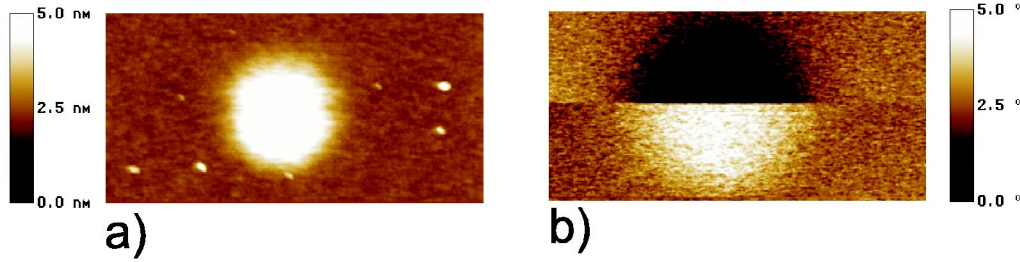

FIG. 3. (Color online) Recorded height (a) and phase (b) data on a thin film of SiO_2 (7 nm) on Si. Scan size is (1×2) μm^2. Charge injection parameters were -10 V and 10 s contact time. The phase is recorded at a lift height of 100 nm. In (b), the tip voltage during lift mode is $V_{EFM}=+2$ V on the upper half of the image, then $V_{EFM}=-2$ V on the lower half. The phase shift jumps from $-3°$ to $+2°$.

film, instead of a metallic surface. If an amount Q of charges is deposited on the surface, a potential V_Q can be associated as

$$V=V_{EFM}-V_Q,$$

$$\text{where}\quad V_Q=\frac{Q}{C}=\frac{Qd_1}{\epsilon_0\epsilon_{SiO_2}S}, \tag{8}$$

and where ϵ_{SiO_2} is the dielectric constant of silicon dioxide and d_1 is the silicon dioxide thickness. This corresponds to an additional capacitance whose plates are the oxide surface and the silicon substrate. Consequently, the extrema in height and phase are not anymore attained for $V_{EFM}=0$ but for $V_{EFM}=V_Q$, still maintaining the above mentioned amplitude feedback and scanning across the voltage applied on the tip. The measurement of V_Q gives access to the number of charges injected locally on the surface. In the case of the plane capacitor model, the relation with the total charge Q is straightforward.[17] In addition, an inhomogeneous charge distribution will show effects on both topography and phase images because V_Q value depends on the sample position.

III. EXPERIMENTAL SETUP

Experiments were performed on a commercial AFM Nanoscope III Dimension 3100 from Veeco Instruments, Santa Barbara, CA, to which a glove box has been added to control the atmosphere. A permanent flux of nitrogen ensures a humidity rate of 15% at ambient temperature in order to avoid the contamination of the sample surface and lithography processes[28] during the charge injection procedure via the AFM tip. A dc voltage, ranging from -12V to $+12$V, can be applied on the tip.

The cantilevers used are manufactured by MikroMasch, Tallinn (Estonia), are of rectangular shape, 35 μm in width, and 90–130 μm in length. Nominal spring constants range from 0.6 to 3 $\mathrm{N\,m^{-1}}$ and resonant frequencies from 75 to 155 kHz (manufacturer's values). Tips are silicon coated with W_2C to ensure a metallic behavior. The nominal radius is 35 nm.

The samples used are silicon dioxide layers thermally deposited on a silicon substrate. The experiments presented were carried out on 7-nm-thick SiO_2 layer. The results are similar on a layer of 25-nm of SiO_2 (data not shown).

As mentioned in the preceding section, only the phase allows determining the regime of operation (intermittent or noncontact). Moreover, the relatively high quality factor of the cantilever in air (here 100–300) ensures a steep variation of the phase vs frequency near the resonance. Thus, the phase signal provides high sensitivity to small variations in the tip-sample interaction. Recording the phase while imaging requires a double-pass method (interleave imaging mode) so as to get rid of topographical artifacts and short-range forces when probing the electrostatic interaction. First, topographical data are recorded in a trace-retrace scan line, while the feedback loop maintains the amplitude of oscillation constant by adjusting the tip-surface distance. In a second step, phase variations are measured by lifting the tip above the surface, switching off the amplitude feedback and performing a second trace and retrace record. Lift scan height used in all the presented experiments is set to 100 nm.

IV. RESULTS AND DISCUSSION

Analytical dynamic force curves provide a qualitative understanding of scan images of charged areas in noncontact mode. In such an experiment, charges are first deposited by stopping the scan and bringing the tip into contact with a dielectric surface for a few seconds while applying a voltage of -10 V. As shown in Fig. 3(a) the sample displays an apparent height on a large area around the position of charging, although it was ''flat'' prior to contact with the tip, with a roughness amounting to less than 1 nm. Charges deposited on the sample surface are equivalent to a voltage applied on the tip, as seen in Fig. 2. When probing the electrostatic forces during the topography scan, the tip has to retract to keep the assigned amplitude setpoint marked in Fig. 2(a).

Furthermore, at a lift height of 100 nm, the phase is influenced both by the presence of the charges and by the tip voltage V_{EFM} [Fig. 3(b)]. An inversion of the phase shift is clearly observed as the tip voltage is switched from $+2$ V to -2 V halfway through the scan. For $V_{EFM}=+2$ V and electrons deposited on the sample surface, the difference $(V_{EFM}-V_Q)$ is positive and larger than the voltage over the uncharged region V_{EFM}. The phase shift being proportional to $-V^2$ [see Fig. 2(d)], the phase lag increases compared to the uncharged region [darker area in Fig. 3(b)]. For $V_{EFM}=-2$ V, the situation is inversed: here $(V_{EFM}-V_Q)$ is

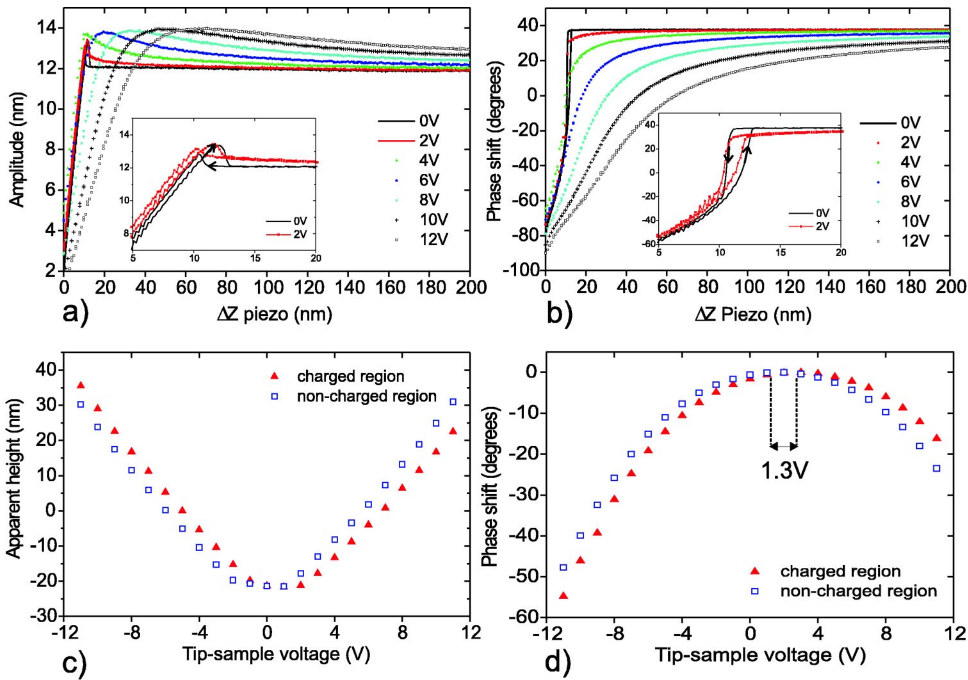

FIG. 4. (Color online) Experimental dynamic force curves over a thin SiO_2 (7 nm) on Si substrate. Since the absolute position of the surface is not known, only relative piezo displacements (Δz) are recorded. (a) and (b) are, respectively, plots of the amplitude and phase of oscillation vs Δz for different voltages applied on the tip. The insets are magnified plots of the hysteretic region at 0 and 2 V, the arrows show the piezo displacement direction. (c) and (d) correspond, respectively, to the apparent height and phase shift as a function of the tip-sample voltage, each for a charged and a noncharged region.

negative and smaller than V_{EFM} in absolute value. Therefore, the phase lag decreases compared to the uncharged region [brighter area in Fig. 3(b)]. This inversion of contrast due to charges of either same or opposite sign in the tip and the sample is also considered in Ref. 17.

Experimental dynamic force curves obtained on uncharged silicon dioxide in noncontact mode with different tip-sample voltages allow significant insights. Results are shown in Fig. 4. Approach-retract curves for amplitude and phase of oscillation have been recorded for different tip-sample voltages ranging from 0 to 12 V in Figs. 4(a) and 4(b), respectively. These curves are in good agreement with the analytical solutions presented in Fig. 2. In particular, these curves display the loss of the hysteresis with increasing voltage. The hysteresis is shown on the magnified plots of the insets for 0 and 2 V tip voltages. The long-range region exhibits a deviation from the analytical plots, with an interaction still detectable as far as 200 nm, whereas theory predicts that at such a distance, amplitude and phase have returned to their free oscillation values. This can be related to a limitation of the plane capacitor model, since the effective plate area is only valid on a small vertical range. At larger tip-sample distances, the effective area should be larger.

In addition, apparent height and phase shifts are plotted against tip-sample voltage in Figs. 4(c) and 4(d), respectively, over a charged and a noncharged region. In the case of the charged surface, charges are first deposited by stopping the scan and bringing the tip into contact during 10 s while applying a voltage of -10 V. Then, scanning is resumed with, however, the slow scan axis disabled, so as to remain over the charges. The same linear behavior for the apparent height and the parabolic behavior for the phase shift are observed as in the analytical solutions. If the parabolic behavior is well explained in the case of the plane capacitor,[17] the linear increase of the height remains unclear.

In Figs. 4(c) and 4(d), the minima of the curves are

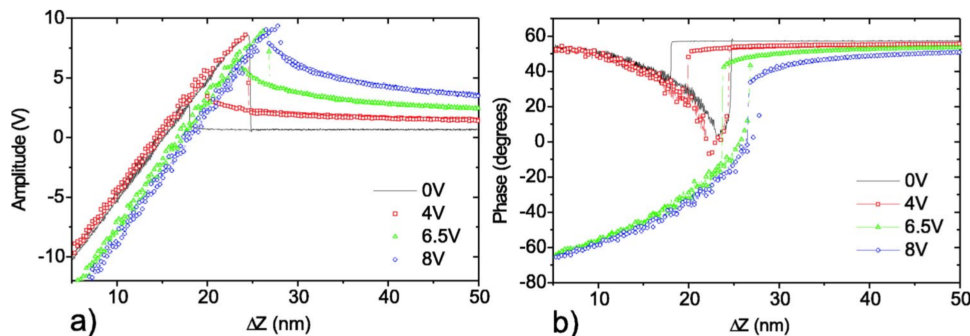

FIG. 5. (Color online) (a) Amplitude and (b) phase of oscillation vs vertical piezo displacement for increasing tip-sample voltage. At 0 V, and until 5 V, the tip is in intermittent contact, as can be seen from the characteristic behavior of the phase. For larger voltages, the state of oscillation suddenly changes to the noncontact regime, and is then governed by electrostatic forces. This process is reversible: when the voltage is set back to zero, the oscillation returns to intermittent contact regime.

shifted by $V=1.3$ V for the charged area. From this value, and using the plane-plane capacitance model with circular plates of 100 nm in diameter, we estimate the amount of detected charges to be $Q=360$ electrons.

To get an idea of the electrostatically induced artifacts in standard imaging applications, it is important to estimate the influence of the attractive, electrostatic interaction on the intermittent contact regime. Figure 5 shows experimental dynamic force curves over an uncharged area of silicon dioxide sample. The initial state, at $V_{EFM}=0V$, is intermittent contact, characterized by the increase of the phase lag with decreasing distance. As the voltage is progressively increased to 5 V, a transition to noncontact regime is observed. This behavior is reversed when the voltage is reduced to zero again. Applying a voltage, a longer-range electrostatic interaction is introduced, damping the amplitude of oscillation of the tip to its setpoint further away from the surface than before [Fig. 2(a)]. In consequence, the tip stops touching the surface and a sharp transition from intermittent to noncontact can be observed in the phase. This experiment highlights the fact that local surface charges can have drastic consequences on the working regime of an AFM, and thus on the phase contrast during imaging. It emphasizes the difficulty of phase contrast interpretation, and underlines the necessity to always check the working conditions of the AFM with dynamic force curves.

V. CONCLUSION

This paper shows the significance of dynamic force curves in atomic force microscopy, in the presence of electrostatic forces. Using a variational method in noncontact regime, and introducing an additional electrostatic term, the oscillating tip's motion is analytically resolved as a function of tip-sample separation. Amplitude and phase exhibit a nonlinear behavior expressed as a hysteresis between the approach and retract curves. However, this hysteresis is lost as the long-range interaction is introduced via a tip-sample voltage. All analytical results are in good agreement with the experiments, and allow determining the amount of injected charges on a surface, using a plane capacitor model. Moreover, these results explain very well the apparent height observed on charged surfaces, and point to phase contrast artifacts due to changes in the working mode of the AFM in the presence of surface charges. All this emphasizes the importance of using dynamic force curves when imaging in ‘‘tapping’’ mode to control the regime of operation.

ACKNOWLEDGMENTS

The authors are grateful to M. Stark for fruitful discussions and critical reading of the manuscript. Also, M. Derivaz, P. Noé, and A. Barski provided many samples made by MBE useful to the understanding of electrostatic forces with the AFM.

*Electronic address: dianoux@esrf.fr
†Electronic address: marchi@polycnrs-gre.fr

[1] G. Binnig, C. Quate, and C. Gerber, Phys. Rev. Lett. **56**, 930 (1986).
[2] R. Carpick and M. Salmeron, Chem. Rev. (Washington, D.C.) **97**, 1163 (1997).
[3] J. Cleveland, B. Anczykowski, A. Schmid, and V. Elings, Appl. Phys. Lett. **72**, 2613 (1998).
[4] J. Tamayo and R. Garcia, Appl. Phys. Lett. **71**, 2394 (1997).
[5] P. Grütter, T. Jung, H. Heinzelmann, A. Wadas, E. Meyer, H.R. Hidber, and H. Guentherodt, J. Appl. Phys. **67**, 1437 (1990).
[6] B. Terris, J. Stern, D. Rugar, and H. Mamin, Phys. Rev. Lett. **63**, 2669 (1989).
[7] P. Girard, M. Ramonda, and D. Saluel, J. Vac. Sci. Technol. B **20**, 1 (2002).
[8] Q. Zhong, D. Innis, K. Kjoller, and V. Elings, Surf. Sci. Lett. **290**, L688 (1993).
[9] S. Watanabe, K. Hane, M. Ito, and T. Goto, J. Appl. Phys. **2573**, 63 (1993).
[10] M. Nelson, P. Schroeder, R. Schlaf, and B. Parkinson, J. Vac. Sci. Technol. B **17**, 1354 (1999).
[11] J. Colchero, A. Gil, and M. Baro, Phys. Rev. B **64**, 245403 (2001).
[12] C. Guillemot, P. Budau, J. Chevrier, F. Marchi, F. Comin, C. Alandi, F. Bertin, N. Buffet, C. Wyon, and P. Mur, Europhys. Lett. **59**, 566 (2002).
[13] E. Boer, L. Bell, M. Brongersma, and H. Atwater, J. Appl. Phys. **90**, 2764 (2001).
[14] M. Vogel, B. Stein, H. Pettersson, and K. Karrai, Appl. Phys. Lett. **78**, 2592 (2001).
[15] T. Melin, D. Deresmes, and D. Stievenard, Appl. Phys. Lett. **81**, 5054 (2002).
[16] L. Klein and C. Williams, Appl. Phys. Lett. **81**, 4589 (2002).
[17] D. Schaadt, E. Yu, S. Sankar, and E. Berkowitz, Appl. Phys. Lett. **74**, 472 (1999).
[18] X. Chen, C. Roberts, J. Zhang, M. Davies, and S. Tendler, Surf. Sci. **519**, L593 (2002).
[19] R. Hillenbrand, M. Stark, and R. Guckenberger, Appl. Phys. Lett. **76**, 3478 (2000).
[20] A. Sebastian, M. Salapaka, D. Chen, and J. Cleveland, J. Appl. Phys. **89**, 6473 (2001).
[21] T. Rodriguez and R. Garcia, Appl. Phys. Lett. **80**, 1646 (2002).
[22] S. Magonov, V. Elings, and M. Whangbo, Surf. Sci. **375**, L385 (1997), phase is used to distinguish between surfaces of different stiffness.
[23] D. Sarid, T. Ruskell, R. Workman, and D. Chen, J. Vac. Sci. Technol. B **14**, 864 (1996).
[24] L. Nony, R. Boisgard, and J.-P. Aime, J. Chem. Phys. **111**, 1615 (1999).
[25] S. Hudlet, M. Saint-Jean, C. Guthmann, and J. Berger, Europhys. Lett. **2**, 5 (1998).
[26] S. Belaidi, P. Girard, and G. Leveque, J. Appl. Phys. **81**, 1023 (1997).
[27] J. Israelachvili, *Intermolecular and Surface Forces*, 2nd ed. (Academic, New York, 1991).
[28] F. Marchi, V. Bouchiat, H. Dallaporta, V. Safarov, and D. Tonneau, J. Vac. Sci. Technol. B **16**, 2952 (1998).